# THE SEASONAL VARIATION OF THE EAST KOREAN WARM CURRENT

Yoon, Jong-Hwan
Research Institute for Applied Mechanics, Kyushu University : Associate Professor

https://doi.org/10.5109/6783292

出版情報：Reports of Research Institute for Applied Mechanics. 38 (108), pp.23-36, 1991-09. 九州大学応用力学研究所

Reports of Research Institute for Applied Mechanics
Vol. XXXVIII, No. 108, 1991

# THE SEASONAL VARIATION OF THE EAST KOREAN WARM CURRENT

By Jong-Hwan YOON*

The result by a multi-level numerical model shows a very interesting seasonal change of the East Korean Warm Current. In winter and spring, the East Korean Warm Current becomes a broad current with relatively weak vertical shear. In summer and fall, the East Korean Warm Current becomes narrower with a strong vertical shear and southward counter current. The analytical study by a reduced gravity model explains the mechanism of this interesting seasonal variation and concludes that in winter and spring the East Korean Warm Current stays in a diffusive regime due to the weak density stratification and moves into a viscous regime (the Munk layer) in summer and fall as the density stratification becomes strong.

***Key words*** : Tsushima Current, Diffusive regime, Viscous regime, Third branch, East Korean Warm Current

## 1. Introduction

The East Korean Warm Current simulated in the multi-level numerical model (Yoon[1]) shows a very interesting seasonal change. In summer, it becomes narrower and accompanied by a recirculation and in winter, it becomes broader with no recirculation. There weren't the theory to explain this interesting seasonal change.

Yoon[2] and Kawabe[3] explained the East Korean Warm Current merely as a western boundary current where the $\beta$ and viscous effects are important. They neglected the importance of the stratification in the dynamics of the East Korea Warm Current. Recently Masuda and Uehara[4] investigated the western and eastern boundary layer in a stratified ocean with a simple reduced gravity model where horizontal diffusion of interfacial displacement is taken into

* Associate Professor, Research Institute for Applied Mechanics, Kyushu University.

account in addition to the ordinary vertical diffusion of Newtonian cooling and concluded that the dynamics of the western boundary layers are classified into the *viscous* regime and *diffusive* regimes. The western boundary layer in *a viscous* regime is almost the same as the Munk layer and is accompanied by a recirculation. The one in a *diffusive* regime is a broad layer with no recirculation.

The object of this study is to investigate the validity of the theory by Masuda and Uehara[4] when it is applied to the East Korean Warm Current.

### 1.1. Description of the multi-level model

The model used is a multi-level model described in Bryan[5]. The equations of motion are the Navier-Stokes equations modified by the Boussinesq approximation and the hydrostatic assumption. Molecular viscosity is replaced by a term of harmonic form. The coefficients of horizontal ($A_h$), vertical ($A_v$) eddy

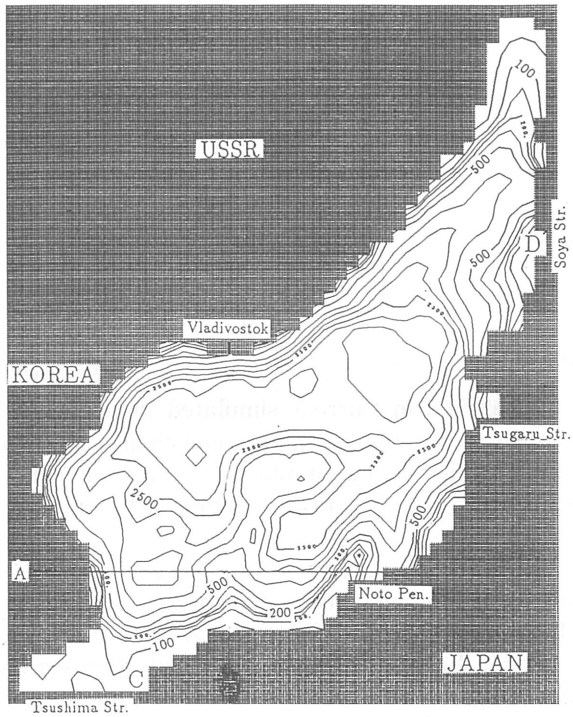


Fig. 1 Bottom topography of the Japan Sea.

viscosity, and thermal diffusivities ($K_h$, $K_v$) are assumed to have constant values: $A_h = 10^7$ cm$^2$/sec, $A_v = 1$ cm$^2$/sec, $K_h = 5\times10^6$ cm$^2$/sec, $K_v = 0.5$ cm$^2$/sec.

The equation of state $\rho = \rho(\theta, S, z)$ is calculated from a nine-term polynomial fit to the Knudsn formula for each vertical level (Bryan and Cox[6]).

At lateral walls, nonslip, no heat and no salt flux are imposed. At the surface,

$$\left.\begin{array}{l} \rho_o A_v(u_z, v_z) = (\tau^\lambda, \tau^\phi) \\ K_v\theta_z = Q/\rho_o C_p \\ K_v S_z = 0 \\ w = 0 \end{array}\right\} \quad at \quad z = 0 \tag{1}$$

where $u$, $v$ and $w$ are velocities in $x$, $y$ and $z$, respectively. And $\theta$ and $S$ are potential temperature and salinity. The rigid-lid assumption of zero vertical motion at the surface filters out high speed external gravity waves. The quantities $\tau^\lambda$, $\tau^\phi$ are the zonal and meridional components of the surface stress, $Q$ (the net upward surface heat flux) is assumed to have the following form $Q = \gamma(\theta_a - \theta_1)$ where $\theta_a$ is the air temperature and $\theta_1$ is the potential temperature of the first level. The coefficient $\gamma$ is taken to be $80 1_y$/day ($\simeq$ 20 day damping time). In this study the wind stress ($\tau^\lambda$, $\tau^\phi$) is taken to be zero. The air temperature $\theta_a$ is deduced from the observed temperature taken from Slutz et al. [7].

The model ocean with a realistic bottom topography shown in Fig. 1 has the grid resolution of 1/3° (longitude, $\delta x$) by 1/3° (latitude, $\delta y$). Vertically there are up to 19 levels. The number of levels at any horizontal position is taken to be that which most closely approximates the depth of the sea at that point. The vertical grid intervals (in meter) with the $T$, $S$, $u$, $v$ points at the center of the grid interval are, from the top level, 15, 15, 20, 25, 30, 35, 35, 35, 50, 75, 100, 150, 200, 300, 450, 600, 600, 600, 600.

### 1.2. Condition of the three straits

We assume the sinusoidal seasonal variation of the volume transport $\psi(t)$ with a minimum in February and a maximum in August as

$$\psi(t) = \psi_0 + A sin\frac{2\pi(t-t_0)}{T} \tag{2}$$

where $T$ = 360 days, $t_0$ = 135 days, $\psi_0 = 2\times10^{12}$ cm$^3$s$^{-1}$, and $A = 0.5\times10^{12}$ cm$^3$s$^{-1}$

The barotropic component of velocity is taken to be constant across the Tsushima Straits. So that the stream function $\psi$ increases linerly toward the east from zero to $\psi(t)$ at the eastern boundary in the Tsushima Straits. The volume transports which flow out through the Tsugaru and the Soya Strait are taken to be $0.7\psi(t)$ and $0.3\psi(t)$, respectively. The baroclinic velocity normal to the inflow boundary in the Tsushima Straits is calculated from the density distribution on the inflow boundary on the assumption of geostrophic relation between these two quantities. The slippery condition is adopted for the velocity tangential to the inflow boundary. The condition for the baroclinic velocities $\hat{\mathbf{u}}$ on the outflow boundaries in the Tsugaru and Sôya Strait is $\hat{\mathbf{u}}_n = 0$, where $n$ denotes the derivative normal to the outflow boundaries.

The imposed seasonal changes in vertical distributions of salinity $S(z, t)$ and reference temperature $T_r(z, t)$ in the Tsushima Straits are determined on the basis of the monthly mean vertical sections of temperature and salinity in the east channel of the Tsushima Straits reported by Nan'niti and Fujiki[8]. Temperature and salinity in winter are uniform vertically. The minimum temperature (13.5°C) occurs in February and the maximum salinity (34.65‰) occurs in April. In summer, vertical stratification develops with a maximum temperature (25.5°C) in September and a minimum salinity (32.7‰) in August in the surface layer.

The initial temperature and salinity are uniform horizontally and the vertical distributions of these values are taken from the values in the central region of the Japan Sea (the East Sea) in early summer.

The time integration starts from the first of January and stops at the end of 127 th year. The upper ocean above 500 m depth repeats almost same seasonal changes after several years time integration. The results of the last year (127 th year) are shown here.

### 1.3. Seasonal variation

Bimonthly vertical sections of temperature along the line A in Fig. 1 are shown in Fig. 2. The main thermocline which is defined as the boundary between the Tsushima Warm Water and the Japan Sea Proper Water is clearly seen in winter around the depth of $150M$ due to the severe winter time cooling. Above the main thermocline, we can see the region of relatively high temperature with the longitudinal width of 2∼3° along the Korean coast where the East Korean Warm Current flows northward. In spring the seasonal thermocline starts to develope and finally the difference between the seasonal and main thermocline disappears in September with the strong horizontal and vertical temperature gradient which suggest the existence of a current with a strong vertical shear. The cooling from the top of the ocean starts from fall destroying the seasonal thermocline with this strong temperature gradient.

Fig. 3 shows bimonthly vertical sections of salinity along the line A in Fig. 1. From March to July, saline water (>34.00‰) occupies the region along the Korean coast with a core in the upper layer shallower than $150M$. The core has the longitudinal width of 2∼3°. In September, the water with low salinity intrudes into the upper thin layer above the saline water forming the salinity maximum in the subsurface with the width of about 2°. During fall and winter the region along the Korean coast are occupied by the low salinity water.

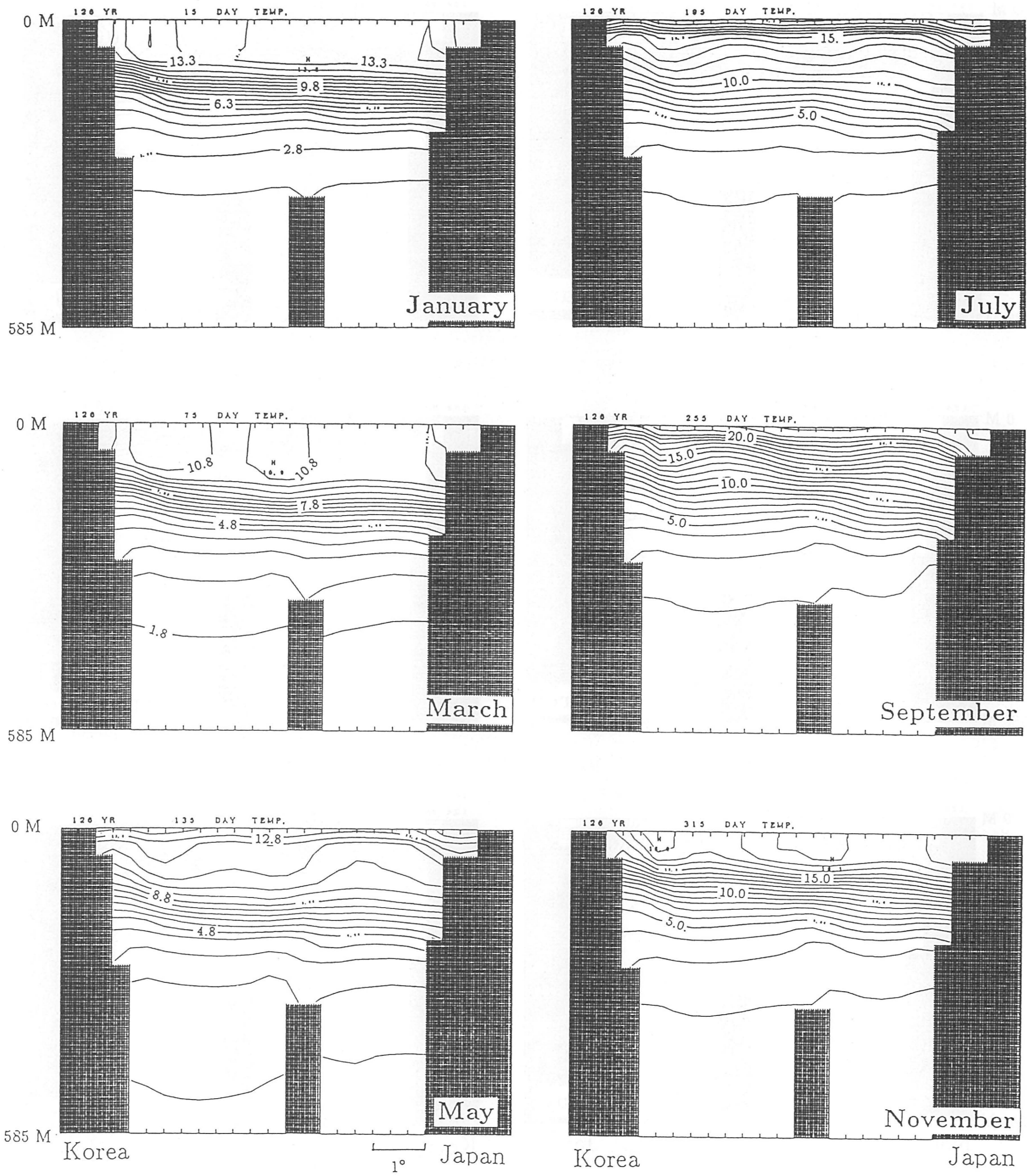


Fig. 2 Bimonthly vertical sections of temperature along the line A in Fig. 1.

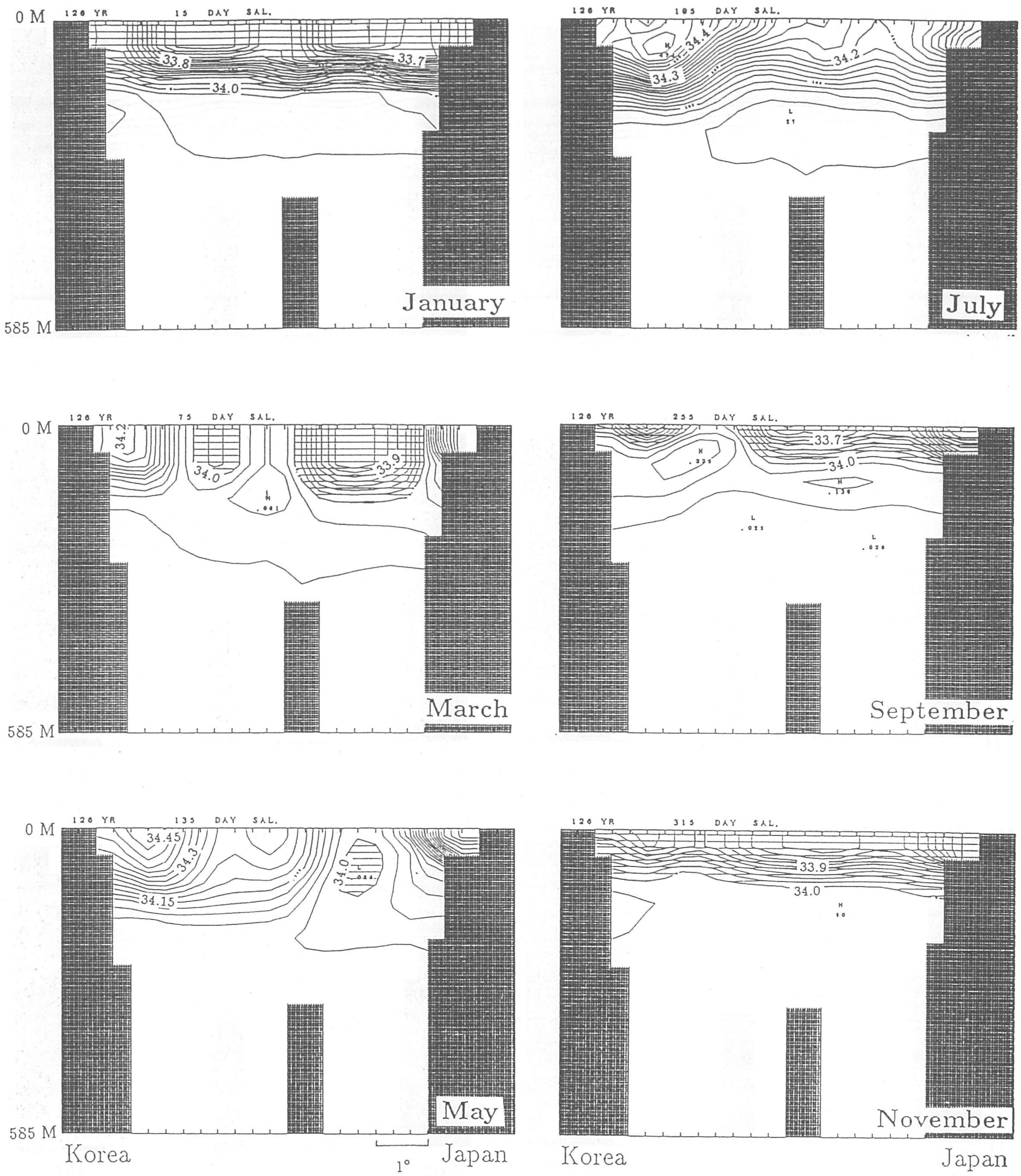


Fig. 3 Bimonthly vertical sections of salinity along the line A in Fig. 1.

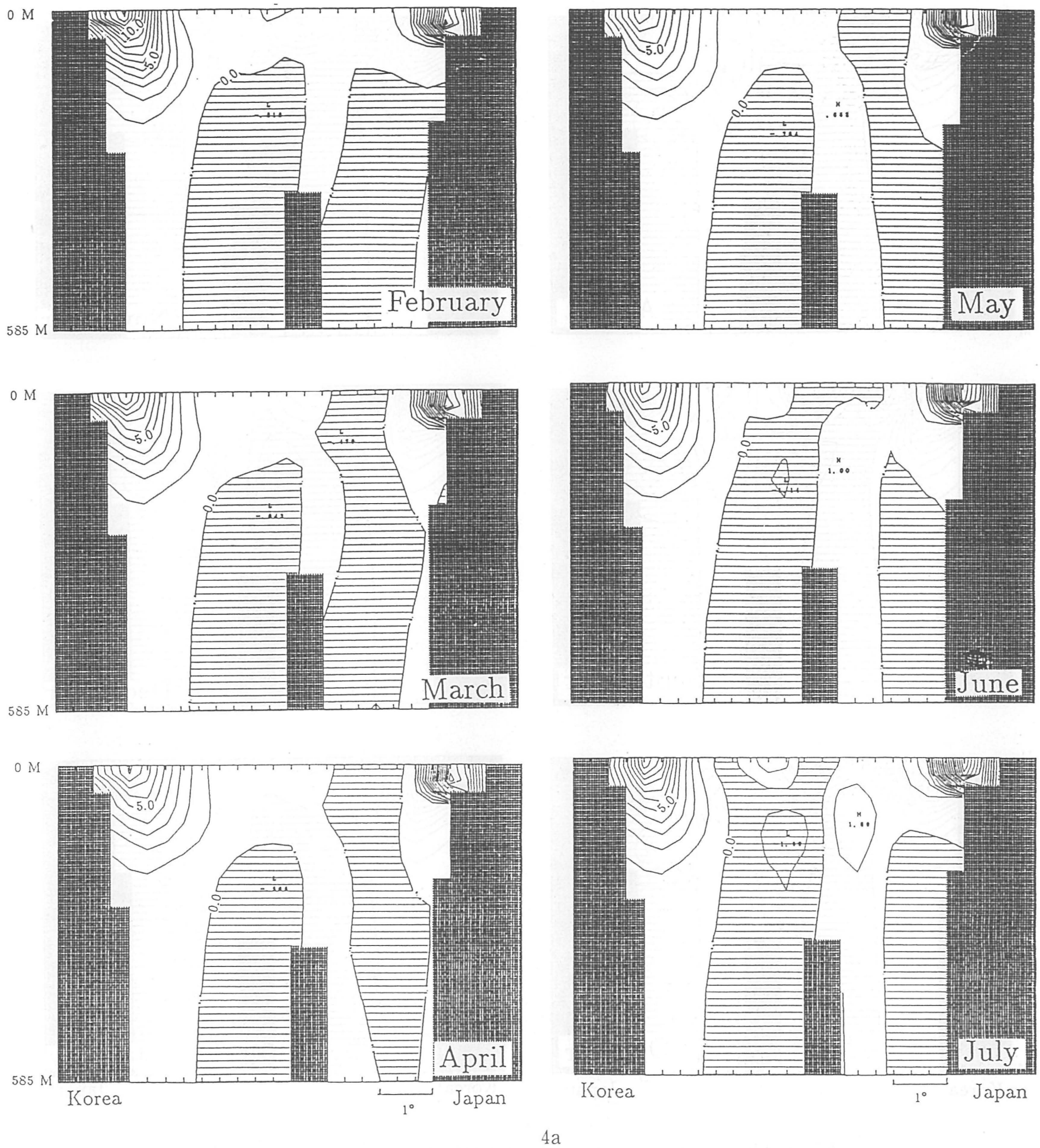
0 M
585 M
February
May
March
June
April
July
10.0
5.0
0.0
Korea
Japan
1°

4a

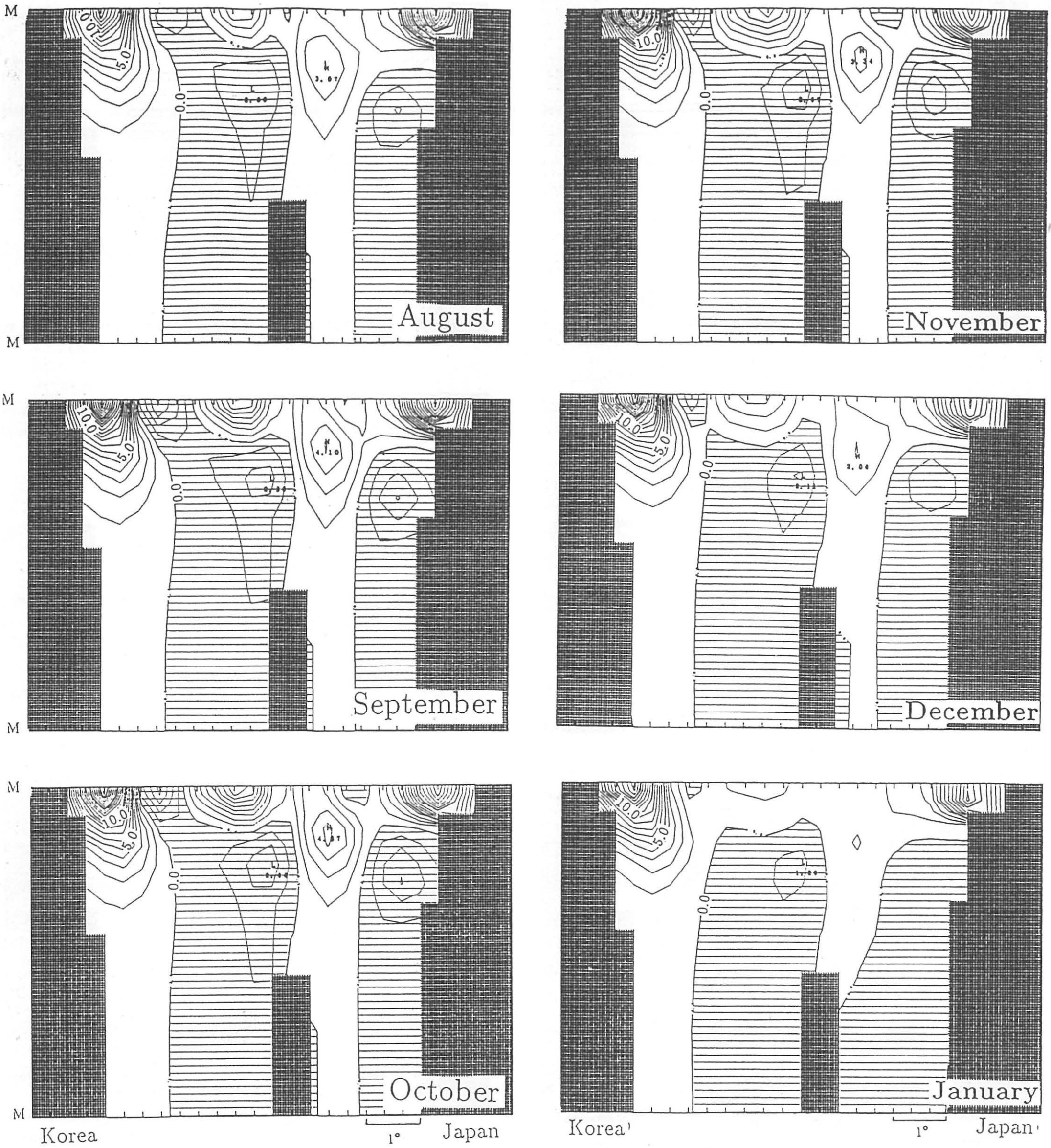


4b

Fig. 4 Bimonthly vertical sections of northward velocity along line A in Fig. 1.

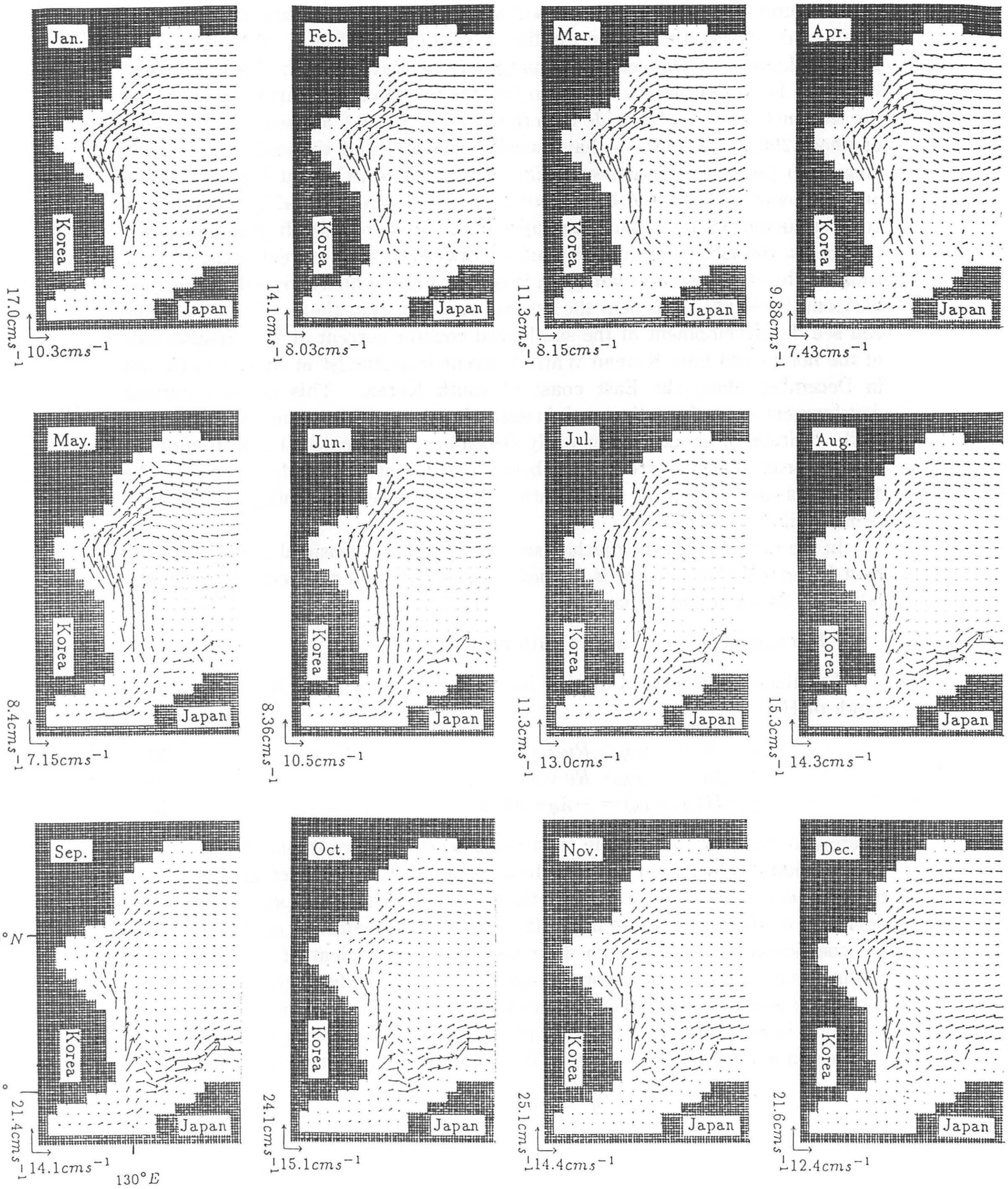


Fig. 5 Monthly variations of the baroclinic horizontal velocity fields at the depth of 7.5$M$ near the east coast of Korea.

It will be very difficult to discuss the details of the current structure from these figures of temperature and salinity. Let's see the vertical sections of northward velocity field along the line A in (Fig. 1) in Fig. 4. We can see the striking feature of the seasonal change of the East Korean Warm Current. From the 1st in February to the 1st in July the East Korean Warm Current along the Korean coast becomes wide with the width of about 2° and with the thickness of about $200M$ and tends to have weak horizontal and vertical shear. From August to January the northward East Korean Warm Current becomes strong and narrower with the width of about 1°20′ and is accompanied by a southward counter current in the surface thin layer at the offshore side. It should be noted that below the subsurface no dominant southward counter currents exist all year round. The same seasonal variation is seen in Fig. 5 which shows the baroclinic horizontal velocity fields near the east coast of Korea at the depth of $7.5M$. We can see the development of the southward counter current at the offshore side of the northward East Korean Warm Current from the 1st in August to the 1st in December along the East coast of south Korea. This counter current development starts from the south in early August and its northern edge extends to the latitude of about $40°N$ in early December. The seasonal variation of the East Korean Warm Current described above might be closely related to the strong seasonal change of stratification due to the severe cooling in winter as seen in Fig. 2.

In the next section the mechanism of this striking seasonal variation of the East Korean Warm Current is studied analytically by a reduced gravity model following Masuda and Uehara[4].

## 2. Mechanism of seasonal variation

The linear equations of motion for a homogeneous upper layer of uniform depth of H :

$$u_t - fv = -g'\eta_x - Ru + \nu\nabla^2 u \quad (3)$$

$$v_t + fu = -g'\eta_y - Rv + \nu\nabla^2 v \quad (4)$$

$$\eta_t + H(u_x + v_y) = -\lambda\eta + \varkappa\nabla^2\eta \quad (5)$$

where $t$ is time, $(x, y)$ are the (eastward, northward) coordinates, $(u, v)$ the corresponding velocities, $f$ the coriolis parameter, $g'$ the reduced gravity due to the small density difference between the lower (quiet) and the upper layer, $\eta$ the deviation of thickness of the upper layer from the mean thickness. $R$ denotes the coefficient of the Rayleigh drag and $\lambda$ the coefficient of the Newtonian cooling (warming). The second dissipative term on the right hand side of continuity equation, which is introduced by Masuda and Uehara[4], is interpreted as the horizontal mixing of mass (isopicnal mixing). Following the formulation of Masuda and Uehara[4], we obtain the following equation for a steady state:

$$\beta\eta_x + (R - \nu\nabla^2)\nabla^2\eta - \ell^2_d(\lambda - \varkappa\nabla^2)\eta = 0 \quad (6)$$

where $R$ and $\nu$ are assumed to be much smaller than $f$.

Assuming $\eta \propto exp(\ell^{-1}x)$ and $\ell_s = \ell/\ell_d$ where $\ell_d = \sqrt{g'H}$ is the radius of deformation, the fourth-order algebraic equation for $\ell_s^{-1}$ near the western and eastern boundaries becomes

$$1-\left(\frac{R}{\lambda}+\frac{\kappa}{\lambda \ell_d^2}\right)\ell_s^{-2}+\frac{\nu}{\lambda \ell_d^2}\ell_s^{-4} = \frac{\beta \ell_d}{\lambda}\ell_s^{-1} \tag{7}$$

It is noted that $\ell_s^{-1}$ with negative real part corresponds to the western boundary layer and positive to the eastern. Since we are interested in only the western boundary layer only the roots with negative real parts are discussed hereafter.

When the quadratic coefficient of (7), $R+\kappa/\ell_d^2$ is small the western boundary scales ($\ell_s$) become complex and recirculation would occur; This type of layer is called a *viscous* western layer (almost the same that of Munk[9]. If $R+\kappa/\ell_d^2$ is large, the western scales are real; the (dimensional) broader scale is

$$\ell_s^{broad} \simeq \frac{R+\ell_d \kappa}{\beta} \tag{8}$$

and the narrower

$$\ell_s^{narrow} \simeq \sqrt{\frac{\nu}{\ell_d^2 R+\kappa}}\,\ell_d \tag{9}$$

This layer with negative real roots is called the *diffusive* layer, where $\kappa$ is important, following Masuda and Uehara [4].

Thus the western boundary layers are thus classified into the viscous and diffusive regimes. The criterion dividing the two regimes are given by

$$\sqrt{\frac{3\nu}{\kappa}}\,\ell_d = \left(\frac{2\nu}{\beta}\right)^{\frac{1}{3}} \tag{10}$$

In this study, the coefficients of Newtonian cooling ($\lambda$), Rayleigh damping ($R$), horizontal viscosity ($\nu$) and diffusivity ($\kappa$) are assumed to have constant values: $\lambda = 10^{-7}\,\mathrm{sec}^{-1}$, $R = 10^{-7}\,\mathrm{sec}^{-1}$, $\nu = 10^{7}\,\mathrm{cm^2 sec^{-1}}$ and $\kappa = 5\times 10^{6}\,\mathrm{cm^2 sec^{-1}}$. Therefore the determination whether the western boundary layer is in the *viscous* regime or *diffusive* regime depends upon only the radius of deformation $\ell_d$. When $\ell_d$ is larger than the critical value $\ell_d^*$ determined by (10), the western boundary layer is in the viscous regime with a recirculation. On the other hand, when $\ell_d$ is less than critical value $\ell_d^*$ the western boundary layer is in the *diffusive* regime.

The equation (7) is solved for various values of the radius of deformation ($\ell_d$). The result is shown in Fig. 6. Four real roots are obtained for a value of $\ell_d$ less than the critical value $\ell_d^*$. For $\ell_d$ larger than the critical value $\ell_d^*$, two positive real roots are obtained and two imaginary solutions with negative real parts are obtained. Averaging the potential $\sigma_t$ horizontally within a distance of 3°(1/3)′ from the Korean coast along the line A in Fig. 1, the mean vertical

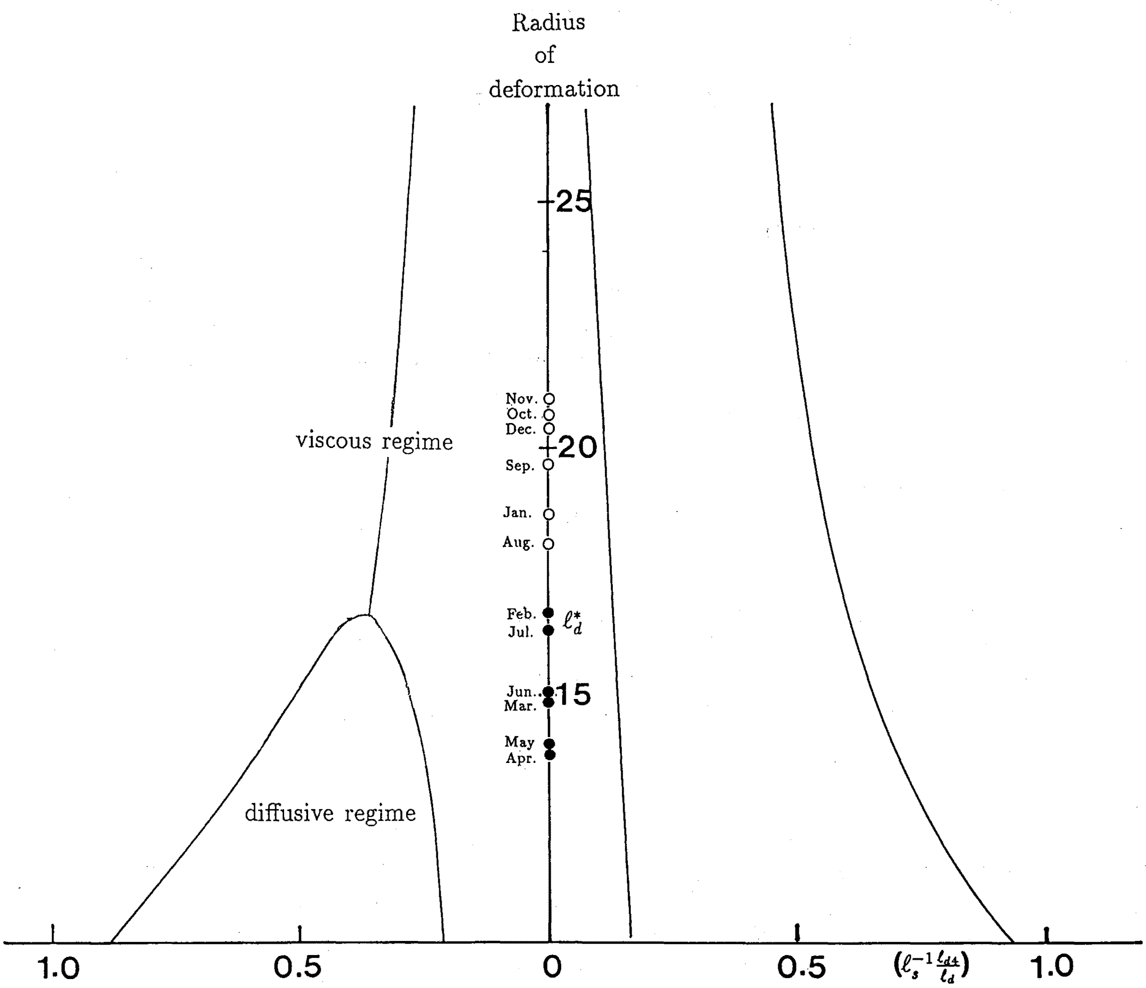


Fig. 6 Solution of the equation (7). The abcissa is the reciprocal of the charcteristic boundary layer length $\ell$ normalized by the radius of deformation $\ell_{d4}$ in April. The ordinate is the radius of deformation. The black dots indicate the months with no southward counter currents at the offshore side and the open circles indicate the months with southward counter currents at the offshore side of the East Korean Warm Current.

profile of potential density is obtained for each month. These continuous vertical profiles of potential density are approximated to the two-layer structures by averaging the density above and below the depth of $105M$. The radius of deformation for each month is calculated by using the density difference and upper layer depth obtained in the way described above. The radius of deformation for each month is indicated in Fig. 6 where the black dots indicate the months with no southward counter current and the open circles indicate the months with southward counter currents at the offshore side of the East Korean Warm Current. We can see the striking coincidence between the theory and the numerical results that the open circles are located above the critical value $\ell_d^*$ (*viscous* regime) and the black dots are located below the critical value $\ell_d^*$ (*diffusive* regime). From the lst in February to the lst in July, as the vertical stability decreases due to the winter time cooling, the radius deformation decreases below the critical value $\ell_d^*$ and the East Korean Warm Current gets into the diffusive regime. From August to January, the East Korean Warm Current moves to the viscous regime as the density stratification becomes strong due to the heating through the ocean surface and the advection of heat by it self.

## 3. conclusion

The results by a multi-level numerical model show a very interesting seasonal change of the East Korean Warm Current. In winter and spring,the East Korean Warm Current becomes a broad current with no recirculation and a relatively weak vertical shear. In summer and fall, the East Korean Warm Current becomes narrower with recirculation (southward counter current) and strong vertical shear. The analytical study by a reduced gravity model explains the mechanism of this interesting seasonal variation and concludes that in winter and spring the East Korean Warm Current stays in a *diffusive* regime due to the weak density stratification and moves into a *viscous* regime (the Munk layer) in summer and fall as the density stratification becomes strong.

These results presented here are only the outputs of the numerical integrations and have to be checked by observations. Nevertheless, these results give a good example for the test of western boundary layer theory in a stratified ocean.

## Acknowledgment

We thank Prof. A. Masuda for valuable discussions and comments during this work.

## References

1) Yoon, J.-H. : *The branching mechanism of the Tsushima Current.*submitted to J. Oceanogr. Soc. Japan

2) Yoon, J.-H. : *Numerical experiment on the circulation in the Japan Sea, Part I Formation of the East Korean Warm Current,* J. Oceanogr. Soc. Japan **38** (1982)

43- 51.

3) Kawabe, M. : *Branching of the Tsushima Current in the Japan Sea. Part* II. *Numerical experiment,* J.Oceanogr. Soc. Japan **38** (1982) 183-192.

4) Masuda, A. and K. Uehara : *A reduced-gravity model of the abyssal circulation with Newtonian cooling and horizontal diffusion.* submitted to Deep-Sea Research.

5) Bryan, K. : *A numerical method for the study of the circulation of the world ocean,* J. Comp. Physic. **4** (1969) 347-376.

6) Bryan, K. and M. Cox : *An approximate equation of state for numerical models of ocean circulation,* J. Phys. Oceanogr. **2** (1972) 510-514.

7) Slutz, J., J. Lubker, J. Hiscoz, S. Woodruff, R. Jenne, D. Joseph, P. Steurer and J. Elms : Comprehensive ocean atmosphere data set. NOAA/ERL, Boulder, CO.

8) Nan'niti, T. and A. Fujiki : *Secular variations of hydrographic conditions in the East Tsushima Strait,* J. Oceanogr. Soc. Japan **23** (1967) 201-212 (in Japanese).

9) Munk, W. H. : *On the wind-driven ocean circulation,* Journal of Meteorology 7 (1950) 79-93.

(Received 12 July, 1991)